Reports of Biochemistry & Molecular Biology
Vol.12, No.3, Oct 2023

Original article

www.RBMB.net

SARS-CoV-2 and Its Omicron Variants Detection with RT-RPA -CRISPR/Cas13a-Based Method at Room Temperature

Jia Li[#1,2], Xiaojun Wang[#1,4], Liujie Chen[1,2], Lili Duan[1,2], Fenghua Tan[1,2], Kai Li[2,3], Zheng Hu*[1,2]

Abstract

Background: The outbreak of severe acute respiratory syndrome coronavirus 2 (SARS-CoV-2) has triggered a global health crisis, with genetic mutations and evolution further creating uncertainty about epidemic risk. It is imperative to rapidly determine the nucleic acid sequence of SARS-CoV-2 and its variants to combat the coronavirus pandemic. Our goal was to develop a rapid, room-temperature, point-of-care (POC) detection system to determine the nucleic acid sequences of SARS-CoV-2 isolates, especially omicron variants.

Methods: Based on the conserved nucleotide sequence of SARS-CoV-2, bioinformatics software was used to analyze, design, and screen optimal enzymatic isothermal amplification primers and efficient CRISPR RNAs (crRNAs) of CRISPR/Cas13a to the target sequences. Reverse transcription-recombinase polymerase amplification (RT-RPA) was used to amplify the virus, and CRISPR/Cas13a-crRNA was used to cleave the SARS-CoV-2 target sequence. The sensitivity of nucleic acid detection was assessed by serial dilution of plasmid templates. All reactions were performed at room temperature.

Results: RT-RPA, combined with CRISPR/Cas13a, can detect the SARS-CoV-2 with a minimum content of 10^2 copies/μL, and can effectively distinguish between the original strain and the Omicron variant with a minimum limit of detection (LOD) of 10^3 copies/μL.

Conclusion: The method developed in this study has potential application in clinical detection of SARS-CoV-2 and its omicron variants.

Keywords: CRISPR/Cas13a, Omicron variants, RT-RPA, SARS-CoV-2.

Introduction

The SARS-CoV-2 outbreak has led to a global health emergency (1), with over 768 million people infected and more than 6.9 million deaths to date. In addition, the virus is constantly evolving and producing new mutant strains, including Alpha, Beta, Gamma, Delta, and Omicron, which are closely monitored by the World Health Organization (WHO) (2). The Omicron variant is highly transmissible and has more than 30 changes in its spike protein (S protein) compared to the original strain (3, 4). This S protein is the main target of immune responses and enables the virus to invade host cells by binding to receptors (5).

1: The First Clinical College of Xiangnan University, the First People's Hospital of Chenzhou Affiliated Xiangnan University, Chenzhou 423000, Hunan, China.
2: Translational Medicine Institute, the First People's Hospital of Chenzhou, Hengyang Medical School, University of South China, Chenzhou 423000, Hunan, China.
3: National Engineering Research Center of Personalized Diagnostic and Therapeutic Technology, Hunan University of Chinese Medicine, Changsha 410208, Hunan, China.
4: The Oncology Department of the First People's Hospital of Chenzhou, Chenzhou 423000, Hunan, China.
#These authors contributed equally to this work.
***Corresponding author: Zheng Hu; Tel: +86 18229336273; E-mail: hu48005@163.com.**
Received: 29 Aug, 2023; Accepted: 14 Jan, 2024

[DOI: 10.61186/rbmb.12.3.425]

The Omicron variant's receptor-binding domain (RBD) is more effective at receptor binding than the original strain due to 15 mutations (6), four of which affect nine key residues and potentially increase the virus's ability to bind hACE2 (7).

Currently, the SARS-CoV-2 detection methods include antigen detection, antibody testing, and nucleic acid molecular detection methods (8, 9). Of these, antigen- and antibody-based rapid tests are the least sensitive, take longer to develop, and may be ineffective in the early/acute infection stages. Reverse transcription-quantitative PCR (real-time RT-PCR) technology is the gold standard for molecular diagnosis. However, the long diagnostic PCR times (typically 4-5 hr), expensive infrastructure instruments, and professional technical operators limit its application. Therefore, there is an urgent need for a point-of-care (POC) detection method with high sensitivity, easy operation and low technical requirements.

To address these limitations, CRISPR/Cas gene editing technology has been explored for nucleic acid detection. Cas proteins such as Cas9, Cas12, Cas13, and Cas14 can be guided by RNA sequences to target and cut specific DNA or RNA molecules (10-17). Among them, Cas9, Cas12, and Cas14 are DNA nucleases, while Cas13 is an RNA nuclease. In addition to their abilities to accurately cleave target nucleic acid sequences, Cas12, Cas13, and Cas14 also have "collateral cleavage" effects. These proteins interact with target sequences. Cas12 targets double-stranded (ds) DNA, Cas14 targets single-stranded (ss) DNA, and Cas13 targets RNA utilizing guide RNA by forming double strands through base complementary pairing, which activates the enzymatic activity of Cas proteins. The “collateral cleavage” effect refers to Cas enzymes being able to cut single-stranded target DNA or RNA molecules non-specifically (16-18). This collateral cleavage can transform target molecules into signal molecules, allowing sensitive and specific nucleic acid detection (19-22).

The detection of nucleic acids using isothermal amplification and collateral cleavage by CRISPR-associated enzymes is an alternative to quantitative PCR. In this study we designed and analyzed the RPA-CRISPR-Cas13a system to detect SARS-CoV-2 RNA and Omicron variants.

Materials and Methods

Preparation of SARS-CoV-2 DNA and RNA targets

The SARS-CoV-2 DNA targets were synthesized and then cloned into the pUC57 plasmid at Genscript Biotech (Nanjing, China). The HiScribe® T7 High Yield RNA Synthesis Kit (E2040S, NEB) was used for in vitro transcription of RNA targets.

crRNA Preparation

For in vitro transcription of crRNA, DNA templates were synthesized by overlapping PCR of two oligos. One oligo contained the T7 promoter sequence and the other contained a spacer sequence. The PCR product was incubated with T7 RNA polymerase for in vitro transcription at 37 °C overnight, and then purified using a miRNeasy Micro Kit (cat 217084, QIAGEN). The crRNA sequences are presented in Table 1.

RT–RPA

Referring to the instructions of the RT-RPA amplification kit (Weifang Amp-Future Biotech), for the 50μL amplification system, 29.4 μL buffer A, 1μL RPA forward primer (10 μM), 1 μL RPA reverse primer (10 μM), and 16.1 μL nuclease-free water were added to the base reaction tube of lyophilized powder, and 2.5 μL of activator was added to the tube after thorough mixing, and then incubated at 39 °C for 20 min. The primer sequences are listed in Table 2.

Five pairs of RPA primers were designed for the SARS-CoV-2 S, ORF1ab, and N genes to select the target sequences for isothermal amplification. Two RPA primer pairs covering the Omicron variant S gene were designed to optimize isothermal amplification of target sequences. The target sequences were amplified via RT-RPA with different RPA primer pairs, then subjected to agarose gel

[DOI: 10.61186/rbmb.12.3.425]

electrophoresis. The primers with distinct amplification bands and no non-specific amplification were selected. For negative controls, the reactions were set up by replacing the templates with diethyl pyrocarbonate (DEPC) -treated water.

Table 1. crRNA sequences used in this study.

Name	sequences（5'→3'）
T7-crRNA-F	GTAATACGACTCACTATAGGGGATTTAGACTACCCCAAAAACGAAGGGGACTAAAAC
S-crRNA-R1	CAGACTCAGACTAATTCTCCTCGGCGGGGTTTTAGTCCCCTTCG
S-crRNA-R2	TCAGACTAATTCTCCTCGGCGGGCACGTGTTTTAGTCCCCTTCG
S-crRNA-R3	TTCTCCTCGGCGGGCACGTAGTGTAGCTGTTTTAGTCCCCTTCG
ORF1ab-crRNA-R1	TCCGCGAACCCATGCTTCAGTCAGCTGAGTTTTAGTCCCCTTCG
ORF1ab-crRNA-R2	CCCATGCTTCAGTCAGCTGATGCACAATGTTTTAGTCCCCTTCG
N-crRNA-R1	GGGGAACTTCTCCTGCTAGAATGGCTGGGTTTTAGTCCCCTTCG
N-crRNA-R2	GGTGATGCTGCTCTTGCTTTGCTGCTGCGTTTTAGTCCCCTTCG
N-crRNA-R3	GATTGAACCAGCTTGAGAGCAAAATGTCGTTTTAGTCCCCTTCG
Spike371-375-WT-R1	TATATAATTCCGCATCATTTTCCACTTTGTTTTAGTCCCCTTCG
Spike371-375-Mut-R1	TATATAATCTCGCACCATTTTTCACTTTGTTTTAGTCCCCTTCG
Spike371-375-WT-R2	ATATAATTCCGCATCATTTTCCACTTTTGTTTTAGTCCCCTTCG
Spike371-375-Mut-R2	ATATAATCTCGCACCATTTTTCACTTTTGTTTTAGTCCCCTTCG
Spike477-478-WT-R1	TCTATCAGGCCGGTAGCACACCTTGTAAGTTTTAGTCCCCTTCG
Spike477-478-Mut-R1	TCTATCAGGCCGGTAACAAACCTTGTAAGTTTTAGTCCCCTTCG
Spike477-478-WT-R2	CTATCAGGCCGGTAGCACACCTTGTAATGTTTTAGTCCCCTTCG
Spike477-478-Mut-R2	CTATCAGGCCGGTAACAAACCTTGTAATGTTTTAGTCCCCTTCG
Spike493-498-WT-R1	TCCTTTACAATCATATGGTTTCCAACCCGTTTTAGTCCCCTTCG
Spike493-498-Mut-R1	TCCTTTACGATCATATAGTTTCCGACCCGTTTTAGTCCCCTTCG
Spike493-498-WT-R2	CCTTTACAATCATATGGTTTCCAACCCAGTTTTAGTCCCCTTCG
Spike493-498-Mut-R2	CCTTTACGATCATATAGTTTCCGACCCAGTTTTAGTCCCCTTCG

Table 2. Primer sequences used in this study

Name	sequences（5'→3'）
pUC57-F	CGAATGCATCTAGATATCGG
pUC57-R	TTACGCCAAGCTTGCATGCA
S-RPA-F1(T7)	GAAATTAATACGACTCACTATAGGGAGGTTTCAAACTTTACTTGCTTTACATAGA
S-RPA-R1	TCCTAGGTTGAAGATAACCCACATAATAAG
S-RPA-F2(T7)	GAAATTAATACGACTCACTATAGGGTTCTAATGTTTTTCAAACACGTGCAGGCTGTTT
S-RPA-R2	ATAGTGTAGGCAATGATGGATTGACTAGCTA
N-RPA-F1(T7)	GAAATTAATACGACTCACTATAGGGAAATTCAACTCCAGGCAGCAGTAGGGGAACTT
N-RPA-R1	CTTGTTGTTGTTGGCCTTTACCAGACATTTTG
N-RPA-F2(T7)	GAAATTAATACGACTCACTATAGGGATCACGTAGTCGCAACAGTTCAAGAAATTCAA
N-RPA-R2	TGCCGAAAGCTTGTGTTACATTGTATGCTTTA
ORF1ab-RPA-F1(T7)	GAAATTAATACGACTCACTATAGGGGTTTTACACTTAAAAACACAGTCTGTACCGT
ORF1ab-RPA-R1	ATTGTGCATCAGCTGACTGAAGCATGGGTT
RPA-S371-375-F(T7)	GAAATTAATACGACTCACTATAGGGCAACTGTGTTGCTGATTATTCTGTCCTATA
RPA-S371-375-R1	TATTTCCAGTTTGCCCTGGAGCGATTTGTC
RPA-S371-375-R2	AGTTTGCCCTGGAGCGATTTGTCTGACTTCA

[DOI: 10.61186/rbmb.12.3.425]

Cas13a-based detection assay

The Cas13a-CRISPR RNA complex binds specifically to the amplified targets RNA and triggers collateral activity, resulting in cleavage of RNA reporters. These cleaved reporters can be detected through fluorescence signals [signal-to-noise (S/N) ratio] or using a colorimetric lateral-flow strip (biotin-fluorescence RNA reporter).

The CRISPR-Cas13a-based detection system is shown in Table 3. Cas13a recombinant protein was purchased from Shanghai HuicH Biotech Co., Ltd (Shanghai, China). The FAM-RNA-biotin reporter (20 μM stock; Genscript, China) and RNase Alert v2 (2 μM stock; Thermo) were used for lateral-flow or fluorescence detection, respectively. The RNA transcribed using RT-RPA products as templates were added as target RNA template to the Cas13a reaction, and then incubated at 37 °C for 30 min.

Table 3. CRISPR/Cas13a detection system for this study

Cas13a detection system（20μL）	volume/μL
Tris-Cl (400 mM, pH 7.4)	2
$MgCl_2$ (120 mM)	1
Cas13a (1 μM)	1
Recombinant RNase Inhibitor (40 U/μL)	0.5
T7 RNA Polymerase (50 U/μL)	0.6
A/C/G/UTP (100 mM)	0.2/each
RNA-probe	1
crRNA (22.5 nM)	1
template	1
DEPC treated water	11.1

After incubation, for lateral-flow detection, 80 μL of HybriDetect assay buffer was added, then samples were mixed, and HybriDetect strips (Milenia Biotech) were inserted for 5 min. The results were observed at last. The appearance of a test band (T) indicated a positive result. For fluorescence detection, fluorescence values were measured on a Varioskan microplate reader (Thermo, wavelength 490 nm, emitted light wavelength 520 nm). High S/N ratio indicated high targeting activity.

To screen out the efficient crRNAs for Spike (S), open reading frame 1ab (ORF1ab), and Nucleocapsid (N) genes, the activity of crRNAs was confirmed by in vitro digestion of target RNAs. Briefly, the RNA transcribed in vitro was used as a template to detect the activity of crRNA-guided CRISPR/Cas13a cleavage of SARS-CoV-2 RNA, and the reaction products were subjected to RNA denatured gel electrophoresis.

Compared to electrophoresis, fluorescence method was faster, more intuitive, and didn't require opening of the lid, so it did not cause secondary contamination. To select the crRNA with highest activity to target SARS-CoV-2 variant Omicron, we mixed Cas13a and different crRNAs with their targeted RNA fragments with variant sites synthesized in vitro and used a fluorescence labeled RNA as report for reaction in 37 ℃. 12 specific crRNAs were designed. These included S-371L/373P/375F (Mut-crRNA 1,2), S-477N/478K/484A (Mut-crRNA 3,4) and S-493R/496S/498R (Mut-crRNA 5,6) for the Omicron variant S gene, and S-371S/373S/375S (WT-crRNA 1,2), S-477S/478T/484E (WT-crRNA 3,4) and S-493Q/496G/498Q (WT-crRNA 5,6) for the original S gene to specifically detect SARS-CoV-2 mutant strains. The reaction which RNA fragment replaced with DEPC water was taken as negative control.

Sensitivity of the RT-RPA/CRISPR–Cas13a assay

Sensitivity of the RT-RPA/CRISPR–Cas13a assay for SARS-CoV-2 RNA or SARS-CoV-2 variant Omicron RNA detection, was investigated by the diluted RNA template using background-subtracted fluorescence readout in final values at 30 min or lateral-flow readout at 30 min.

RNA expression assay (Real-time RT-PCR detection)

The activity of crRNA was verified by clinical samples. Prior to real-time RT-PCR, the SARS-CoV-2 RNA of clinical samples reacted

[DOI: 10.61186/rbmb.12.3.425]

with the CRISPR/Cas13a cleavage system. The samples treated with system without Cas13a enzyme were used as control samples. According to the product instructions, the processed RNA was amplified by 2019-nCoV Nucleic Acid Diagnostic Kit, a commercial real-time RT-PCR kit to detect SARS-CoV-2 ORF1ab and N gene (Sansure Biotech, Changsha, China).

Clinical nucleic acid samples

In 2020, the nasopharyngeal swabs of two patients infected SARS-CoV-2 who confirmed by real-time RT-PCR detection in clinical laboratory of the First People's Hospital of Chenzhou were extracted for viral nucleic acid testing. In 2022, the nasopharyngeal swabs of nine SARS-CoV-2 positive patients with Omicron variant verified in clinical laboratory of the First People's Hospital of Chenzhou were extracted for viral nucleic acid testing. The remaining nucleic acid samples after the detection of clinical laboratory were approved by the Ethics Committee of the First People's Hospital of Chenzhou for the research of new nucleic acid detection methods based on nucleic acid isothermal amplification and CRISPR-Cas technology. Furthermore, the clinical samples with Omicron variant were confirmed by sequencing using the amplification products of RT-RPA.

Results

Optimization of Cas13a-mediated detection

By analyzing the gene sequence of SARS-CoV-2, three target genes were selected. These were Spike (S), ORF1ab, and Nucleocapsid (N) (Fig. 1A). Three S gene crRNAs (crRNA-S1, crRNA-S2, crRNA-S3), and two ORF1ab crRNAs (crRNA-ORF1ab1, crRNA-ORF1ab2), and three N gene crRNAs (crRNA-N1, crRNA-N2, crRNA-N3) were designed. Through RNA denatured gel electrophoresis, the results showed after treated with crRNA/Cas13a, the amount of SARS-CoV-2 RNA were obviously decreased compared to control group, implicating RNA templates were cut by Cas13a effectively. Of these eight crRNAs, the targeting activity of crRNA-S2, crRNA-ORF1ab-1, and crRNA-N3 were greatest (Fig. 1B).

Then, we adopted crRNA-S2, crRNA-ORF1ab-1, and crRNA-N3 to detect different SARS-CoV-2 gene regions. The activity of these crRNAs was confirmed through fluorescence readout. The S/N ratios of the test groups (with crRNA) were significantly greater than those of the control groups (without crRNA), indicating these crRNAs can guide Cas13a to cut the targeted RNA sequence of SARS-CoV-2 efficiently (Fig. 1C).

Furthermore, the activity of these crRNAs was verified by SARS-CoV-2 clinical samples. RNA of two SARS-CoV-2 clinical samples reacted with the CRISPR/Cas13a cleavage system prior to real-time RT-PCR. After reacting with CRISPR/Cas13a cleavage system, the RNA expression levels of S, Orf1ab, and N gene of SARS-CoV-2 were detected by real-time RT-PCR, and the results showed the RNA levels were much less than those of the control groups (Figs. 1D & 1E). Together, these results indicate that these three crRNAs have specificity and higher activity for guiding Cas13a to targeted cleave SARS-CoV-2 RNA.

RT-RPA combined with Cas13a-mediated detection to detect SARS-CoV-2

RT-RPA was used to amplify and enrich the targeted RNA fragment of SARS-CoV-2. Follow RT-RPA, the amplified sequence was converted to RNA in vitro by transcription and was used as template to be cut by Cas13a and crRNA, triggering the incidental cleavage effect of the reporter molecule, which was detected by fluorescent or lateral flow strips (Fig. 2A).

To optimize the RT-RPA primer pairs, we designed several different RPA primer pairs crossing the crRNAs binding region for amplification of S and Orf1ab genes of SARS-CoV-2 according to the RPA primer rules and used the targeted RNA sequences of SARS-CoV-2 as template to amplify by RT-RPA. Then the products of RT-RPA were subjected to agarose gel electrophoresis. As shown in Fig. 2B the amplification bands of lanes 2 and

[DOI: 10.61186/rbmb.12.3.425]

5 were evident and there was no non-specific amplification, indicating that these two primer pairs for the Spike gene (RPA primer set 2) or ORF1ab (RPA primer set 5) had the best amplification efficiency. Based on comprehensive consideration, RPA primer set 2 and crRNA-S2 targeting S gene were selected for follow-up experiments.

To evaluate the sensitivity of RT- RPA combined with Cas13a, gradient-diluted synthetic SARS-CoV-2 RNA templates (10^{11}, 10^{10}, 10^{8}, 10^{6}, 10^{4}, and 10^{2} copies/μL) and two clinical RNA samples of SARS-CoV-2 were tested. The fluorescence and strip assays based on RT-RPA combined Cas13a/crRNA system have shown that this method can detect templates as low as 10^{2} copies/μL, and clinical samples were also detected (Figs. 2C & 2D).

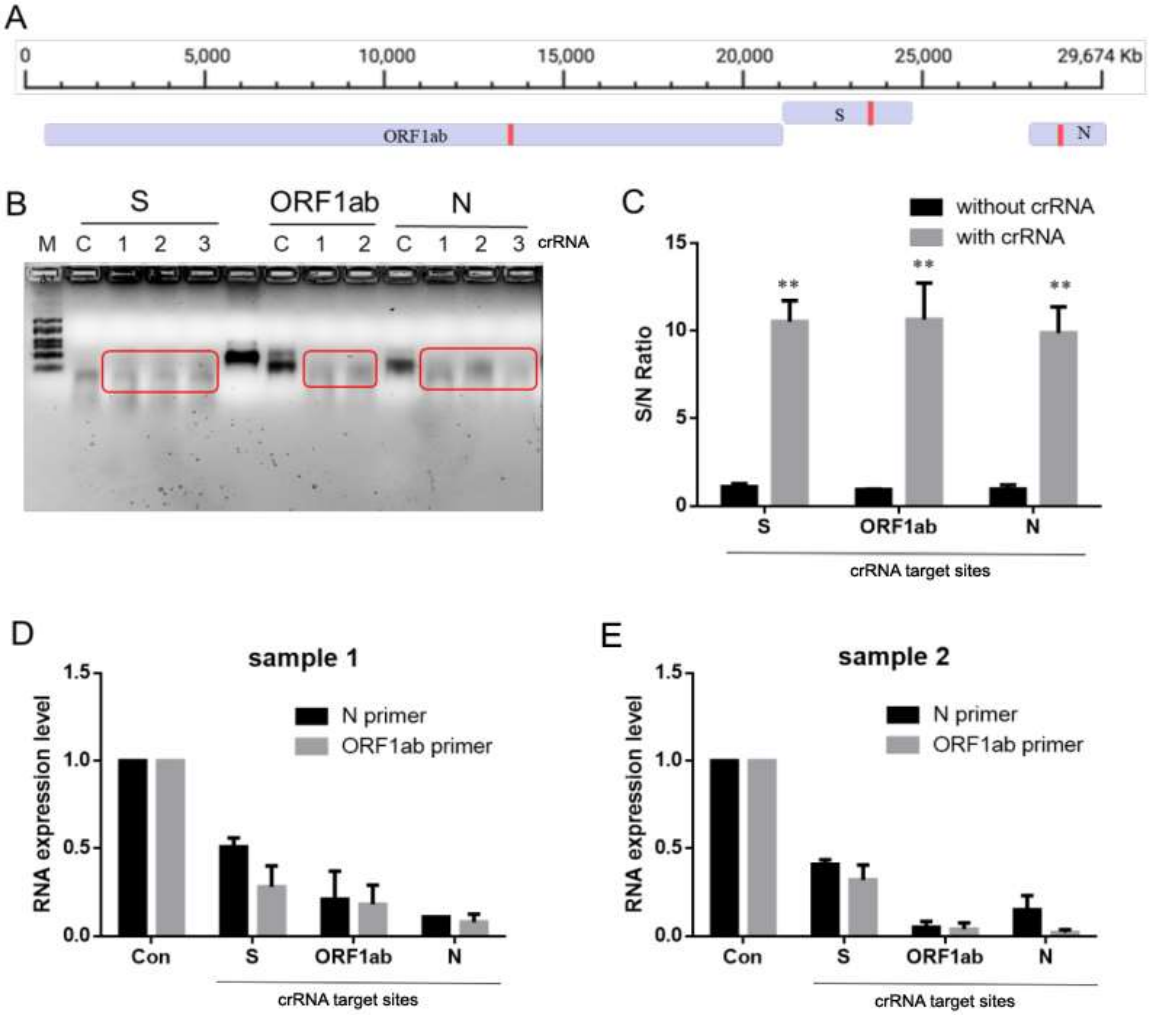

Fig. 1. Optimization of Cas13a-mediated detection. (A) SARS-CoV-2 representative genome. Three targets (red bars) were selected for detection on the SARS-CoV-2 genome. ORF1ab, S, Spike. N, nucleocapsid genes of SARS-CoV-2. (B) *In vitro* cleavage assay of various crRNA samples for S, ORF1ab, and N genes. The RNA synthesized in vitro was used as a template to detect the activity of crRNA-guided CRISPR/Cas13a cleavage of SARS-CoV-2 RNA, and the reaction products were subjected to RNA denatured gel electrophoresis. C, control, treated with a cleavage system without plus crRNA. (C) Identification of crRNA-S2, crRNA-ORF1ab1 and crRNA-N3 through CRISPR/Cas13a trans-cleavage of the fluorescence reporter. The S/N ratios of the test groups (with crRNA) were significantly greater than those of the control groups (without crRNA), indicating that the targeting activity of these crRNAs was high. (D, E) RNA expression levels of SARS-CoV-2 RNA extracts from two clinical samples. SARS-CoV-2 RNA from clinical samples reacted with the CRISPR/Cas13a cleavage system prior to real-time RT-PCR test. According to the product instructions, the processed RNA was amplified by a commercial real-time RT-PCR kit for SARS-CoV-2 ORF1ab, N gene (2019-nCoV Nucleic Acid Diagnostic Kit). Con, control group, the samples treated with cleaved system without Cas13a enzyme. Signal-to-noise (S/N) of fluorescence intensities: with noise being the fluorescence intensity from a negative sample with water as input performed in parallel.

[DOI: 10.61186/rbmb.12.3.425]

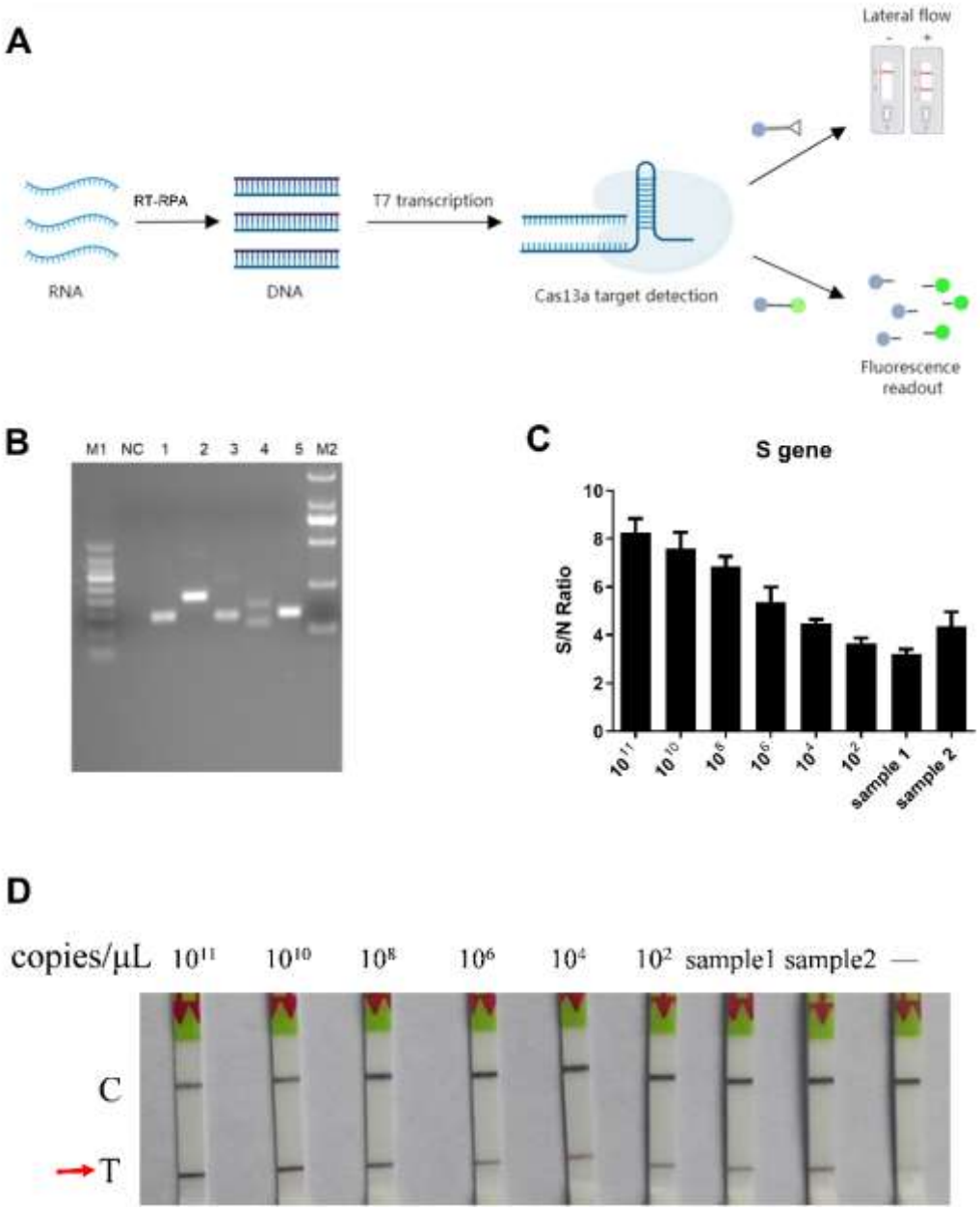

Fig. 2. RT-RPA combined with Cas13a-mediated detection to detect SARS-CoV-2. (A) Schematic of Cas13a-mediated detection. The SARS-CoV-2 RNA region of interest is amplified to DNA using RT-RPA (reverse transcription recombinase polymerase amplification), which is then converted back to RNA via T7 transcription. The Cas13a-CRISPR RNA complex binds specifically to the amplified RNA targets and triggers collateral activity, resulting in cleavage of RNA reporters. These cleaved reporters can be detected through fluorescence signals or using a colorimetric lateral-flow strip (biotin-fluorescence RNA reporter). This approach enables sensitive and reliable detection of SARS-CoV-2 RNA in a rapid and efficient manner. (B) Selection of RPA primers for SARS-CoV-2. The target sequences of SARS-CoV-2 were amplified via RT-RPA with different RPA primer pairs, then subjected to agarose gel electrophoresis. S-RPA-F2/S-RPA-R2 was selected because of the strong brightness of the amplification band. Lane M1, 50bp DNA Marker; Lane NC, Negative control (RNase-free water as the input template for RPA); Lanes 1 and 2 (for Spike gene fragments), S-RPA-F1/S-RPA-R1and S-RPA-F2/S-RPA-R2 respectively; Lanes 3 and 4 (for N gene fragments), N-RPA-F1/N-RPA-R1 and N-RPA-F2/N-RPA-R2 respectively; Lane 5 (for ORF1ab gene fragments), ORF1ab-RPA-F1/ORF1ab-RPA-R1 (all from Table 2); Lane M2: 100bp DNA Marker. (C, D) Sensitivity of the RT-RPA/CRISPR–Cas13a assay for SARS-CoV-2 detection, was investigated by the diluted RNA template from 2×10^{11} to 2×10^{2} copies/μL using background-subtracted fluorescence readout in final values at 30 min (C) or lateral-flow readout at 30 min (D). Signal-to-noise (S/N) of fluorescence intensities, with noise being the fluorescence intensity from a negative sample with water as input performed in parallel. The red arrowhead indicates the expected band appearance at T (test line). C, control line. Green arrows indicate the flow direction.

[DOI: 10.61186/rbmb.12.3.425]

Cas13a-mediated detection of SARS-CoV-2 variant Omicron

Compared with the original strain of SARS-CoV-2, the Omicron variant has more than 30 mutations in the S protein, with RBD having the most mutations. Fig. 3A shows the mutation sites in the Alpha, Beta, Gamma, Delta, and Omicron variant S protein RBD regions. We focused on these mutations, which differ from those of other variants.

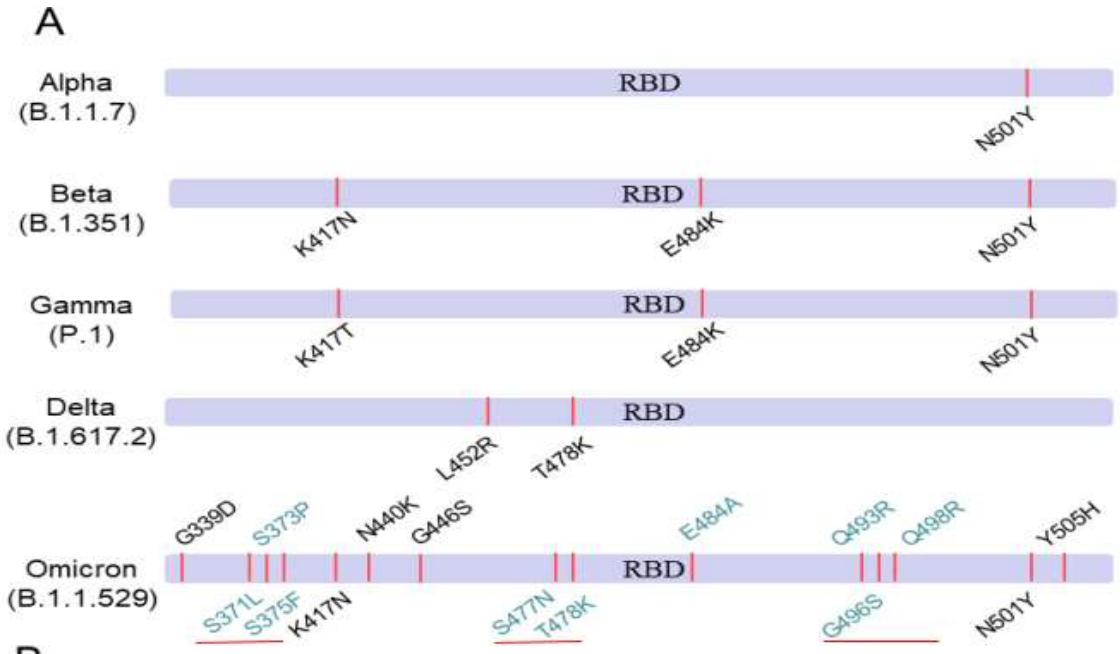

B

WT S gene (371S, 373S, 375S)	5'-CCTATATAATTCCGCATCATTTTCCACTTTTAA-3'
Mut S gene (371L, 373P, 375F)	5'-CCTATATAATCTCGCACCATTTTTCACTTTTAA-3'
WT-crRNA1	5'-UAUAUAAUUCCGCAUCAUUUUCCACUUU-3'
Mut-crRNA1	5'-UAUAUAAUCUCGCACCAUUUUUCACUUU-3'
WT-crRNA2	5'-AUAUAAUUCCGCAUCAUUUUCCACUUUU-3'
Mut-crRNA2	5'-AUAUAAUCUCGCACCAUUUUUCACUUUU-3'
WT S gene (477S, 478T)	5'-AATCTATCAGGCCGGTAGCACACCTTGTAATG-3'
Mut S gene (477N, 478K)	5'-AATCTATCAGGCCGGTAACAAACCTTGTAATG-3'
WT-crRNA3	5'-UCUAUCAGGCCGGUAGCACACCUUGUAA-3'
Mut-crRNA3	5'-UCUAUCAGGCCGGUAACAAACCUUGUAA-3'
WT-crRNA4	5'-CUAUCAGGCCGGUAGCACACCUUGUAAU-3'
Mut-crRNA4	5'-CUAUCAGGCCGGUAACAAACCUUGUAAU-3'
WT S gene (493Q, 496G, 498Q)	5'-TTTCCTTTACAATCATATGGTTTCCAACCCAC-3'
Mut S gene (493R, 496S, 498R)	5'-TTTCCTTTACGATCATATAGTTTCCGACCCAC-3'
WT-crRNA5	5'-UCCUUUACAAUCAUAUGGUUUCCAACCC-3'
Mut-crRNA5	5'-UCCUUUACGAUCAUAUAGUUUCCGACCC-3'
WT-crRNA6	5'-CCUUUACAAUCAUAUGGUUUCCAACCCA-3'
Mut-crRNA6	5'-CCUUUACGAUCAUAUAGUUUCCGACCCA-3'

Fig. 3. crRNA design of mutation sites in Omicron variant Spike protein RBD regions. (A) Schematic diagram of mutation sites in the Spike protein RBD region of the Alpha, Beta, Gamma, Delta, and Omicron variants. (B) Schematic of target regions and the crRNA sequences used for detection.

For these mutation sites, 12 specific crRNAs were designed. These included S-371L/373P/375F, S-477N/478K/484A and S-493R/496S/498R for the Omicron variant S gene, and S-371S/373S/375S, S-477S/478T/484E and S-493Q/496G/498Q for

[DOI: 10.61186/rbmb.12.3.425]

the original S gene to specifically detect SARS-CoV-2 mutant strains (Fig. 3B).

To select the crRNA with highest activity to target SARS-CoV-2 variant Omicron, we mixed Cas13a and different crRNAs with their targeted RNA fragments with variant sites synthesized in vitro and used a fluorescence labeled RNA as report for reaction in 37 ℃. The results showed that the fluorescence intensity of crRNA1 and crRNA2 was six times that of the negative control group, and the crRNAs designed for S-371/373/375 effectively recognized target sequences (Figs. 4A & 4B), where only mutation crRNA1 [Mut-crRNA1 (S-371L/373P/375F)] specifically distinguished between the original strain S gene and the Omicron variant S gene (Figs. 5A & 5B).

We designed RPA primers covering the Omicron variant S gene to optimize isothermal amplification of target sequences, and selected RPA-set1 to proceed the next experimental step due to its strong RPA amplification for SARS-CoV-2 Omicron variants (Fig. 4C).

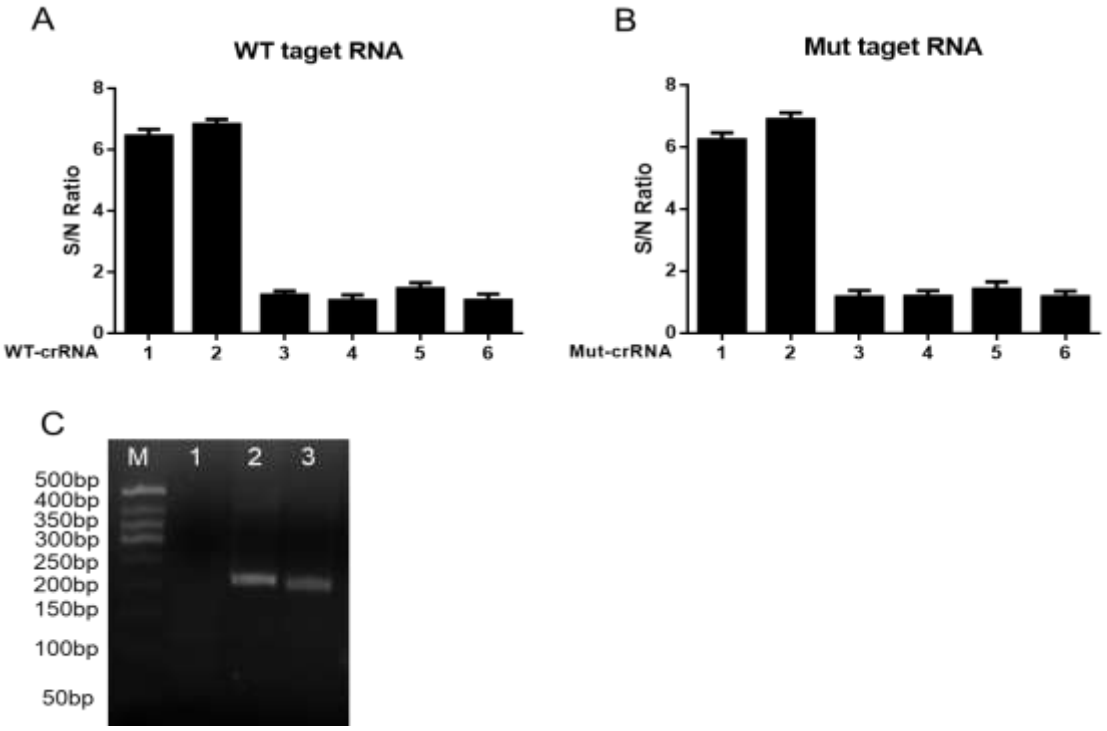

Fig. 4. crRNA and primer selection of SARS-CoV-2 Omicron variants. (A, B) To select the crRNA with highest activity to target SARS-CoV-2 variant Omicron, we mixed Cas13a and different crRNAs with their targeted RNA fragments with variant sites synthesized in vitro and used a fluorescence labeled RNA as report for reaction in 37 ℃. WT-crRNAs and WT target RNA (A). Mut-crRNAs and Mut target RNA (B). The fluorescence intensity of crRNA1 and crRNA2 was six times that of the negative control group, indicating that these crRNAs effectively recognized target sequences. (C) Primer selection. The target sequences were amplified via RT-RPA with different primer pairs, then subjected to agarose gel electrophoresis. RPA-set1 primer pair was selected due to its strong RPA amplification for SARS-CoV-2 Omicron variants (lane 2). Lane1, RPA negative control (RNase-free water used as template); Lane 2, RPA-set1 primer pair; Lane 3, RPA-set2 primer pair.

We combined RT-RPA pre-amplification of viral nucleic acids and the Cas13a-mediated detection. The wild-type S gene was distinguished from the Omicron variant S gene through Mut-crRNAs1 (Figs. 5C & 5D). The limit of detection (LOD) was 10^3 copies/μL.

A validation study was performed with nine clinical samples, including eight real-time RT–PCR-verified SARS-CoV-2-positive samples (Ct range 21–35 for N gene) and one SARS-CoV-2-negative sample. The poor sensitivity of detecting samples using lateral flow (Fig. 5E) at higher Ct values (⩾35) may be due to the need for a critical concentration of cleaved RNA reporter to accumulate sufficient gold nanoparticles to generate an observable colorimetric signal on the test line.

The fluorescence detection result (Fig. 5F)

[DOI: 10.61186/rbmb.12.3.425]

was consistent with clinical real-time RT–PCR results. The results of sequencing further confirmed the mutation sites S-371L/373P/375F of the Omicron variant (Fig. 6).

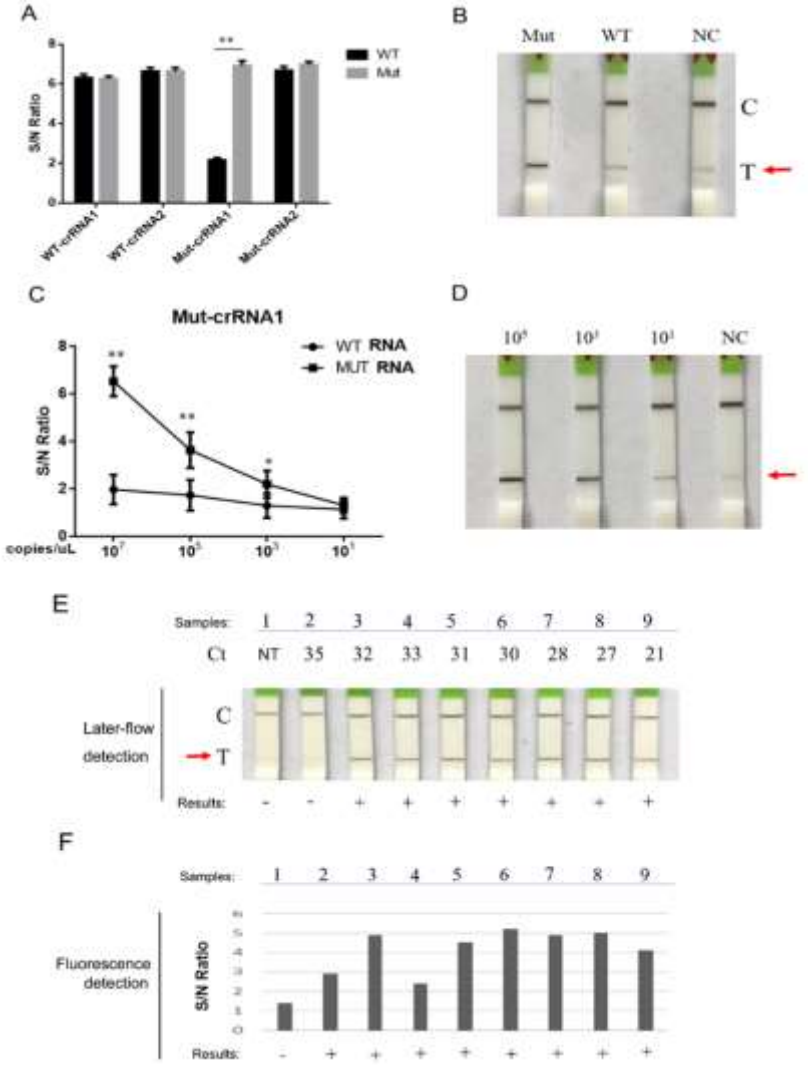

Fig. 5. Cas13a-mediated detection of SARS-CoV-2 variant Omicron. The Cas13a-CRISPR RNA complex binds specifically to the RNA targets and triggers collateral activity, resulting in cleavage of RNA reporters. These cleaved reporters can be detected through fluorescence signals (S/N ratio) or using a colorimetric lateral-flow strip (biotin-fluorescence RNA reporter). (A) crRNA selection from WT-crRNA1-2 and Mut-crRNA1-2 by Cas13a fluorescence-based detection to distinguish between wild and mutant RNA. Three crRNAs activity was high but can't distinguished between WT RNA and Mut RNA. Only mutation crRNA1 [Mut-crRNA1 (S-371L/373P/375F)] specifically distinguished between the original strain S gene and the Omicron variant S gene. (B) Activity validation of Mut-crRNA1 activity through CRISPR/Cas13a lateral flow-based detection. Compared with WT group, Mut group appeared obvious T band. (C) LOD assay of SARS-CoV-2 mutations S-371L, 373P, 375F by Cas13a fluorescence-based detection. (D) LOD assay of SARS-CoV-2 mutations S-371L, 373P, 375F by Cas13a lateral flow-based detection. Synthetic SARS-CoV-2 RNA was diluted to obtain 10^1, 10^3, 10^5 and 10^7 copies/μL. The diluted samples were subjected to RT-RPA using primers (optimized RPA-Set1 shown in Fig. 5C) and followed by Cas13a lateral flow-based detection. Samples with 10^3 copies/μL were easily distinguishable from the sample containing no target RNA. (E, F) Validation of our RT-RPA/CRISPR–Cas13a system for SARS-CoV-2 variant Omicron detection using clinical samples. The detection results are presented as background subtraction, a lateral-flow readout within 30 min (E), or a final fluorescence readout at 30 min (F). For the lateral-flow readout, the appearance of a test band (T) indicated a positive result. For the fluorescence readout, we set the threshold of signal-to-noise (S/N) of fluorescence intensities (with noise being the fluorescence intensity from a negative sample with water as input performed in parallel) for a positive result to be over 2. Ct, Ct values of real-time RT–PCR tested in clinical laboratory; +, indicates a positive sample, −, indicates a negative sample; C, control band; T, test band; NC, no target control; NT, negative test sample.

[DOI: 10.61186/rbmb.12.3.425]

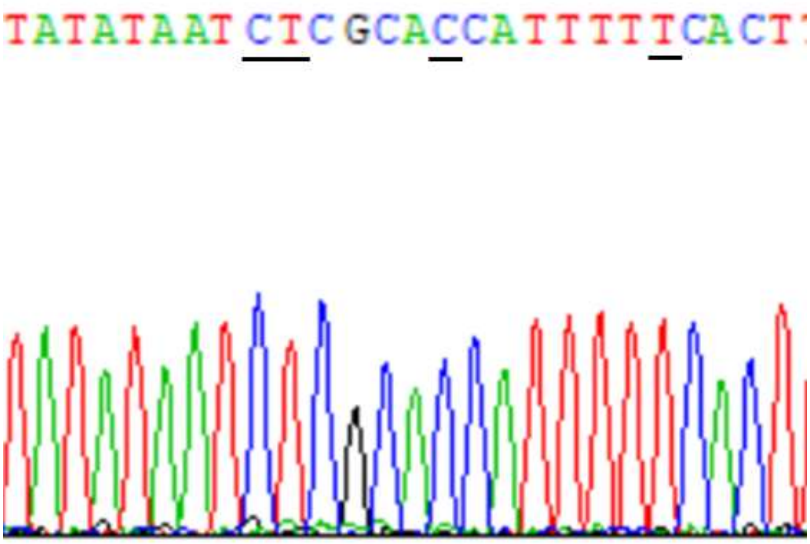

Fig. 6. One representative result of sequencing for Omicron variant clinical samples with mutation sites S-371L/373P/375F. Three out of nine clinical viral nucleic acids samples with Omicron variant (S-371L/373P/375F) were amplified by RT-RPA using RPA-set1 primer pair. The amplification products were purified using DNA product purification kit (TIANGEN, Beijing, China) and subjected to Sanger sequencing. The results of sequencing were confirmed by contrast to SARS-CoV-2 wild type sequence. One representative result of sequencing is shown in this figure.

Discussion

Recently, researchers have detected nucleic acid target sequences using the cleavage activity of CRISPR-Cas. In the CRISPR/Cas13a system, crRNAs are highly targeted, inexpensive to design, and require only 24 bases to cut target RNA by altering the Cas13a protease conformation through the uracil-rich stem-ring structure. However, direct detection using CRISPR methods has low sensitivity and long identification times and is easily affected by sample type (23, 24). Because the detection method combining isothermal amplification and CRISPR has the advantages of high sensitivity and specificity, convenience, rapidity, and efficiency, it is suitable for on-site diagnosis, and many researchers use it to detect SARS-COV2. Fluorescence readings have 100% specificity and sensitivity, while lateral-flow results have 100% specificity and 97% sensitivity (25, 26). Some researchers have used similar methods to detect Spike gene mutation sites., These include K417N/T, L452R/Q, T478K, E484K/Q, N501Y and D614G to distinguish Alpha, Beta, Gamma, and Delta, but not Omicron variants (27-29). The research focus of this study was to detect and distinguish the Omicron variant mutation site.

Our method can be performed using either fluorescence or lateral-flow readings, depending on the purpose of use. Fluorescence readings are better suited for high-throughput assessment, while the lateral-flow readings are better suited for POC usage in the community, airport, or remote area.

However, some shortcomings remain. Multiple crRNAs were designed for multiple sites in the Omicron variant Spike gene RBD region, although only one was highly specific. However, this result showed the method's feasibility.

CRISPR gene editing technology is developing rapidly. Christie et al (30) found that SpRY was less limited by the PAM site in vitro, can cut DNA on almost any sequence, and SpRYgests can broaden the range of various DNA engineering applications that benefit from precise DNA breaks. By applying other CRISPR techniques (Cas12, Cas14, SpCas9 mutants, etc.), it will be possible to find solutions to any new mutation sequence, and more detectable mutation sites.

[DOI: 10.61186/rbmb.12.3.425]

Acknowledgments
We thank Hui Li, Rongzhang He, Tan Tan and Dixian Luo, from the First People's Hospital of Chenzhou, for providing the viral nucleic acid of SARS-COV-2.

Ethics approval and consent to participate
The study was approved by the local Ethics Committee. All experiments were approved by the Ethics Committee of the First People's Hospital of Chenzhou, Hunan, P.R. China, and all patients provided informed consent.

Funding statement
This work was supported by the Natural Science Foundation of Hunan Province (2021JJ30050, 2023JJ50368), Science and Technology Program of Hunan Province (2021SK50313), the Key Science and Technology Program of Chenzhou (ZDYF2020011), and the Inovative Team Project of the First People's Hospital of Chenzhou (CX202103), the Key Project of the First People's Hospital of Chenzhou (CZYY202203), the Health Department Project of Hunan Province (20232204, 202103100449), the Special funding fund for clinical research of Wu Jieping Foundation (grant number 320.6750.19094-25), and the Research Project of Xiangnan University (2019XJ74).

Conflict of interest
The authors declare no conflicts of interests.

References
1. Kadam SB, Sukhramani GS, Bishnoi P, Pable AA, Barvkar VT. SARS-CoV-2, the pandemic coronavirus: Molecular and structural insights. J Basic Microbiol. 2021;61(3):180-202.
2. Hadj Hassine I. Covid-19 vaccines and variants of concern: A review. Rev Med Virol. 2022;32(4):e2313.
3. Meo SA, Meo AS, Al-Jassir FF, Klonoff DC. Omicron SARS-CoV-2 new variant: global prevalence and biological and clinical characteristics. Eur Rev Med Pharmacol Sci. 2021;25(24):8012-8.
4. Thakur V, Ratho RK. OMICRON (B.1.1.529): A new SARS-CoV-2 variant of concern mounting worldwide fear. J Med Virol. 2022;94(5):1821-4.
5. Guruprasad L. Human SARS CoV-2 spike protein mutations. Proteins. 2021;89(5):569-76.
6. Koley T, Kumar M, Goswami A, Ethayathulla AS, Hariprasad G. Structural modeling of Omicron spike protein and its complex with human ACE-2 receptor: Molecular basis for high transmissibility of the virus. Biochem Biophys Res Commun. 2022;592:51-3.
7. Bazargan M, Elahi R. OMICRON: Virology, immunopathogenesis, and laboratory diagnosis. J Genet Med. 2022;24(7):e3435.
8. Dinnes J, Sharma P, Berhane S, van Wyk SS, Nyaaba N, Domen J, et al. Rapid, point- of- care antigen tests for diagnosis of SARS-CoV-2 infection. Cochrane Database Syst Rev. 2022;7(7):CD013705.
9. Ejazi SA, Ghosh S, Ali N. Antibody detection assays for COVID-19 diagnosis: an early overview. Immunol Cell Biol. 2021;99(1):21-33.
10. Mali P, Yang L, Esvelt KM, Aach J, Guell M, DiCarlo JE, et al. RNA-guided human genome engineering via Cas9. Science (New York, NY). 2013;339(6121):823-6.
11. Knott GJ, Doudna JA. CRISPR-Cas guides the future of genetic engineering. Science (New York, NY). 2018;361(6405):866-9.
12. Ali Z, Mahas A, Mahfouz M. CRISPR/Cas13 as a Tool for RNA Interference. Trends Plant Sci. 2018;23(5):374-8.
13. Abudayyeh OO, Gootenberg JS, Konermann S, Joung J, Slaymaker IM, Cox DB, et al. C2c2 is a single-component programmable RNA-guided RNA-targeting CRISPR effector. Science (New York, NY). 2016;353(6299):aaf5573.
14. Smargon AA, Cox DBT, Pyzocha NK, Zheng K, Slaymaker IM, Gootenberg JS, et al. Cas13b Is a Type VI-B CRISPR-Associated RNA-Guided RNase Differentially Regulated by Accessory

[DOI: 10.61186/rbmb.12.3.425]

Proteins Csx27 and Csx28. Mol cell. 2017;65(4):618-30.e7.
15. Wang F, Wang L, Zou X, Duan S, Li Z, Deng Z, et al. Advances in CRISPR-Cas systems for RNA targeting, tracking and editing. Biotechnol adv. 2019;37(5):708-29.
16. Gootenberg JS, Abudayyeh OO. Nucleic acid detection with CRISPR-Cas13a/C2c2. Science (New York, NY). 2017;356(6336):438-42.
17. Gootenberg JS, Abudayyeh OO. Multiplexed and portable nucleic acid detection platform with Cas13, Cas12a, and Csm6. Science (New York, NY). 2018;360(6387):439-44.
18. Teng F, Cui T, Feng G, Guo L, Xu K, Gao Q, et al. Repurposing CRISPR-Cas12b for mammalian genome engineering. Cell discov. 2018;4:63.
19. Caliendo AM, Hodinka RL. A CRISPR Way to Diagnose Infectious Diseases. N Engl J Med. 2017;377(17):1685-7.
20. Kostyusheva A, Brezgin S, Babin Y, Vasilyeva I, Glebe D, Kostyushev D, et al. CRISPR-Cas systems for diagnosing infectious diseases. Methods (San Diego, Calif). 2022;203:431-46.
21. Myhrvold C, Freije CA. Field-deployable viral diagnostics using CRISPR-Cas13. Science (New York, NY). 2018;360(6387):444-8.
22. Chang Y, Deng Y, Li T, Wang J, Wang T, Tan F, et al. Visual detection of porcine reproductive and respiratory syndrome virus using CRISPR-Cas13a. Transbound Emerg Dis. 2020;67(2):564-71.
23. Fozouni P, Son S, Díaz de León Derby M, Knott GJ, Gray CN, D'Ambrosio MV, et al. Amplification-free detection of SARS-CoV-2 with CRISPR-Cas13a and mobile phone microscopy. Cell. 2021;184(2):323-33.e9.
24. Steens JA, Zhu Y, Taylor DW. SCOPE enables type III CRISPR-Cas diagnostics using flexible targeting and stringent CARF ribonuclease activation. Nat Commun. 2021;12(1):5033.
25. Hu F, Liu Y, Zhao S, Zhang Z, Li X, Peng N, et al. A one-pot CRISPR/Cas13a-based contamination-free biosensor for low-cost and rapid nucleic acid diagnostics. Biosens Bioelectron. 2022;202:113994.
26. Joung J, Ladha A, Saito M, Segel M, Bruneau R, Huang MW, et al. Point-of-care testing for COVID-19 using SHERLOCK diagnostics. medRxiv [Preprint]. 2020:2020.05.04.20091231.
27. Liang Y, Lin H, Zou L, Zhao J, Li B. CRISPR-Cas12a-Based Detection for the Major SARS-CoV-2 Variants of Concern. Microbiol Spectr. 2021;9(3):e0101721.
28. Wang Y, Xue T, Wang M, Ledesma-Amaro R, Lu Y, Hu X, et al. CRISPR-Cas13a cascade-based viral RNA assay for detecting SARS-CoV-2 and its mutations in clinical samples. Sens Actuators B Chem. 2022;362:131765.
29. Wang Y, Zhang Y, Chen J, Wang M, Zhang T, Luo W, et al. Detection of SARS-CoV-2 and Its Mutated Variants via CRISPR-Cas13-Based Transcription Amplification. Anal Chem. 2021;93(7):3393-402.
30. Christie KA, Guo JA, Silverstein RA, Doll RM. Precise DNA cleavage using CRISPR-SpRYgests. Nat Biotechnol. 2022;41(3):409-16.

[DOI: 10.61186/rbmb.12.3.425]